SCIENTIFIC REPORTS

OPEN

SUBJECT AREAS:
COMPOSITES
SYNTHESIS AND PROCESSING
BIOMIMETICS
MATERIALS CHEMISTRY

Received
21 May 2013

Accepted
25 October 2013

Published
13 November 2013

Correspondence and requests for materials should be addressed to A.P. (abhay.pandit@nuigalway.ie); D.P.F. (david.finn@nuigalway.ie) or F.D.M. (delmonte@icmm.csic.es)

Integration of TiO_2 into the diatom *Thalassiosira weissflogii* during frustule synthesis

Yvonne Lang[1,3,4], Francisco del Monte[6], Brian J. Rodriguez[5], Peter Dockery[2], David P. Finn[3,4] & Abhay Pandit[1]

[1]Network of Excellence for Functional Biomaterials, [2]Anatomy, School of Medicine, [3]Pharmacology & Therapeutics, School of Medicine, [4]Centre for Pain Research, National Centre for Biomedical Engineering Science National University of Ireland, Galway, Ireland, [5]Conway Institute of Biomolecular and Biomedical Research and School of Physics University College Dublin, Belfield, Dublin 4, Ireland, [6]Instituto de Ciencia de Materiales de Madrid-ICMM Consejo Superior de Investigaciones Científicas-CSIC Campus de Cantoblanco 28049-Madrid, Spain.

Nature has inspired the design of complex hierarchical structures in the field of material science. Diatoms, unicellular algae with a hallmark intricate siliceous cell wall, have provided such a stimulus. Altering the chemistry of the diatom frustule has been explored to expand on the potential application of diatoms. The ability to modify the diatom *in vivo* opens the possibility to tailor the diatom to the end application. Herein, we report the chemical modification of the living diatom *T. weissflogii* using a titania precursor, titanium (IV) bis-(ammonium lactato)-dihydroxide (TiBALDH). Incorporation of Ti into the diatom is achieved *via* repeated treatment of cultures with non-toxic concentrations of TiBALDH. The characteristic architectural features of the diatom are unaltered following chemical modification. Transformation of the living diatom provides opportunity to confer novel structural, chemical or functional properties upon the diatom. We report on a photocatalytic ability imparted upon the TiBALDH-modified diatom.

Diatoms are ubiquitous in seawater and freshwater environments, with the number of species estimated to be between 10^4–10^5 [1]. The complexity and the precision at which the cell wall, the frustule, is synthesised, at both the micro- and nano-scale, is a paradigm among material chemists for the controlled assembly of nanostructured materials[2,3]. Over the past decade there has been a surge of interest in altering the chemistry of the diatom frustule while preserving the intricate architecture. A number of processes have described the use of frustules as sacrificial templates for the generation of non-siliceous diatom replicas[4–7]. Despite the successful use of these processes, an emerging area of particular interest is the alteration of both diatom structure[8] and chemical composition[9–11] in culture.

Advances in chemical manipulation of the living diatom require an understanding of the biomineralization processes that underlie the formation of the intricate valve architecture. The first biomolecules indicated in diatom silica formation are the silaffins[12,13] and long-chain polyamines[14], proteins shown to induce *in-vitro* precipitation of silica from silicic acid[12]. More recently, TiO_2 precipitation has also been induced by silaffins over a wide range of pHs using TiBALDH as a precursor[15]. It was hypothesized that substitution of the natural silica source of diatoms, Na_2SiO_3, with the Ti-based precursor, TiBALDH, will allow incorporation of Ti into the frustule of the centric diatom *Thalassiosira weissflogii* (*T. weissflogii*).

The range of proposed applications for the diatom frustule spans across many disciplines including; catalysis[16], separation science[17–19], optics[20,21], and drug delivery[22–24]. It is always the cleaned harvested diatom that attracts attention and the possibility of harnessing the living diatom has not yet been fully explored.

This manuscript describes a method to alter the chemical composition of the living diatom *T. weissflogii* via Ti substitution. A high level of Ti incorporation is achieved *via* multiple dosing of cultures with concentrations of TiBALDH that satisfy the criteria of non-cytotoxicity and solubility. The chemical modification is not associated with alterations to the pore architecture of the diatom. However, minor changes to the rib structure are observed. Finally, irradiation of TiBALDH-modified diatoms with UV light led to the decay of *Escherichia coli* (*E. coli*) in co-culture demonstrating a novel photocatalytic activity. This property was also indicated when degradation of the photodegradable dye was observed following incubation with cleaned TiBALDH-modifed *T. weissflogii* exposed to UV light.

Results

***T. weissflogii* growth profiles in the presence of TiBALDH.** In this study design it was essential that the concentration of TiBALDH added to the culture medium meets the following balance; (i) it does not adversely affect the growth profile of *T. weissflogii*, and (ii) it does not precipitate in the culture medium. A series of cultures were supplemented with TiBALDH at concentrations ranging from 0.2 mM to 2 mM. Cell density and precipitate formation were monitored daily. TiBALDH concentrations lower than 1 mM were non-toxic to *T. weissflogii* (Figure 1a). Concentrations above 200 μM resulted in the formation of precipitate in the culture media over time. A comparison of the growth profile of *T. weissflogii* cultured in the presence of 200 μM Na_2SiO_3 versus 200 μM TiBALDH shows a similar pattern (Figure 1b) indicating that TiBALDH is not detrimental to *T. weissflogii* growth.

Nutrient depletion of either Na_2SiO_3 or TiBALDH in the culture media leads to a prolonged stationary phase (Figure 1b). Hence; a multiple dosing strategy of adding either Na_2SiO_3 or TiBALDH at 48 hour intervals was investigated to prolong the increased growth. The growth profile of *T. weissflogii* was similar using either precursor; furthermore an extension of increased growth is observed (Figure 1c).

A complete understanding of TiBALDH-associated growth of *T. weissflogii* is limited as the genetic manipulations required to fully investigate the mechanistic pathways are not developed. A specific inhibitor of Ti uptake by *T. weissflogii* or any diatom does not currently exist. Thus, an indirect method of investigating TiBALDH-associated growth involved monitoring growth in the presence of sodium azide, a respiratory inhibitor, that has been shown to inhibit silica uptake and arrest cell division[25,26]. Increases in cell density were reduced significantly when either *T. weissflogii* or TiBALDH-modified *T. weissflogii* were cultured in the presence of 10 mM sodium azide (Figure 1d).

Ti content of *T. weissflogii* frustule. EDX-SEM analysis confirmed that Ti was incorporated into the frustule of TiBALDH-modified *T.*

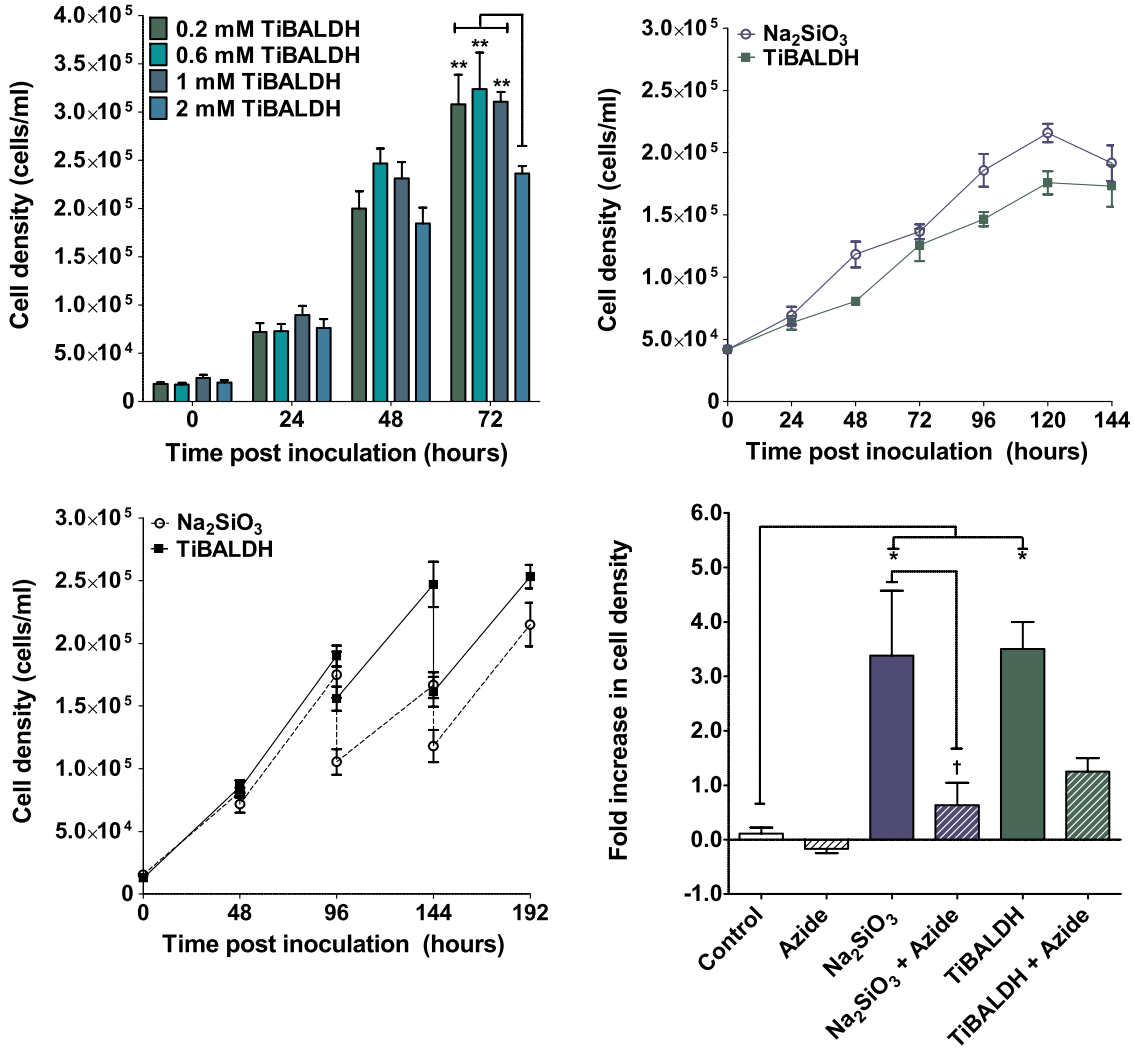

Figure 1 | TiBALDH associated growth profiles of *T. weissflogii*. (a) Increased starting concentrations of TiBALDH did not increase the growth pattern of *T. weissflogii*. Concentrations above 0.2 mM caused the appearance of precipitate in the culture and concentrations above 1 mM adversely affected growth of *T. weissflogii*. Two-way ANOVA revealed an effect of time and treatment. Bonferroni *post-hoc* analysis revealed statistical significance ** $p < 0.01$ ($n = 4$). (b) *T. weissflogii* grown in the presence of TiBALDH only does not adversely affect growth patterns ($n = 3$). (c) Addition of TiBALDH every 48 hours extends exponential growth of *T. weissflogii* compared to a single dose of TiBALDH ($n = 6$). The decrease observed in cell density at 48-hour intervals is due to sampling of cultures following addition of Na_2SiO_3 or TiBALDH. (d) Sodium azide inhibits growth of *T. weissflogii*. In the absence of sodium azide cultures undergo a greater than 2-fold increase in cell density. One-way ANOVA revealed a significant effect of treatment $F_{(5,15)} = 6.787$, $p = 0.0052$ ($n = 3$). Student Newman Keuls *post hoc* analysis ($p < 0.05$) showed statistical difference between Control vs Na_2SiO_3, Control vs TiBALDH, Na_2SiO_3 vs Na_2SiO_3 + Azide. Data are presented as mean ± sem in all panels.

weissflogii (Figure 2). The Ti content was dependent on the number of TiBALDH doses that the culture received. A single addition of TiBALDH at the time of inoculation resulted in a maximum of 8.8 pg Ti/valve at 48 hours and then decreased to ca. 3 pg Ti/valve in the stationary phase (Figure 2a). The replenishment of the TiBALDH precursor in the culture media every 48 hours revealed consistency of Ti content over the period of culturing with maximum content of 13.8 pg Ti/valve after 192 hours following multiple addition of

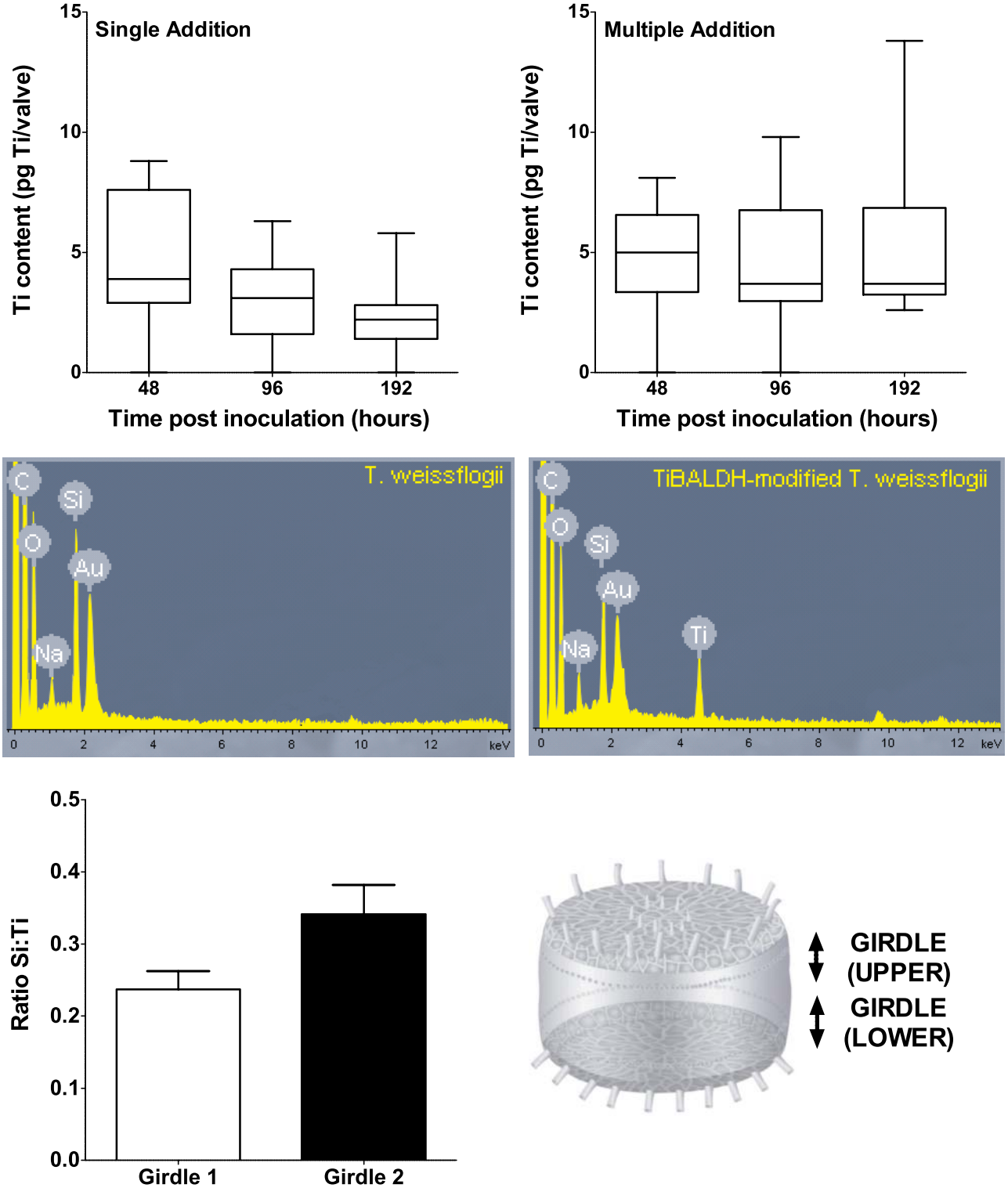

Figure 2 | Investigation of the effect of TiBALDH dosing on Ti content in frustule reveals increases in Ti content is achieved by multiple dosing of cultures every 48 hours. EDX-SEM analysis was performed on the valve of *T. weissflogii* to quantify the ratio of Ti:Si allowing the Ti content per valve to be calculated. Cultures were treated with (a) a single addition or (b) multiple additions of TiBALDH. Data are presented as median and IQR with minimum and maximum values ($n = 12$). EDX-SEM spectra of (c) *T. weissflogii* showing a Si signal and (d) TiBALDH-modified *T. weissflogii* showing both a Si and Ti signal. (e) Incorporation of titanium into the frustule of *T. weissflogii* results in a gradient of titanium content across the girdle view. Data are represented as mean ± sem ($n = 9$). *t*-test revealed a statistical difference between Girdle 1 and Girdle 2. (f) Schematic illustrating the division of upper and lower girdle for analysis of Ti gradient across the girdle view by EDX-SEM analysis.

TiBALDH (Figure 2b). ICP-MS analysis corroborates this result revealing a Ti content of 14.2 ± 5.1 pg Ti per valve. In addition, the quantity of biogenic silica in the TiBALDH-modified *T. weissflogii* frustule is reduced in comparison to the unmodified diatom, with values of SiO_2 per frustule of 28 pg and 51 pg respectively.

EDX-SEM measurements across the girdle band revealed the existence of a gradient in Ti content (Figure 2e). The weight ratio of Ti : Si gave values of 0.24 : 1 compared 0.34 : 1 between bands. The distinction between bands is illustrated schematically in Figure 2f. EDX-TEM analysis of 90 nm thick cross sections of *T. weissflogii* and TiBALDH-modified *T. weissflogii* further confirmed the presence of Ti within the frustule of the modified diatom (Figure 3a & 3c). These observations suggest that Ti incorporation is growth associated as depicted in Figure 4. Furthermore, EDX-SEM analysis confirmed the absence of Ti in the frustule of *T. weissflogii* cultured in the presence of TiBALDH and sodium azide (Supplementary Figure 1). XPS analysis performed on a bulk sample of the TiBALDH-modified diatom confirmed the chemical form of Si and Ti present as SiO_2 and TiO_2 (Figure 3b & 3d).

Architectural parameters of TiBALDH-modified *T. weissflogii*. *T. weissflogii* is a centric diatom measuring 10–15 μm in diameter with a central ring of fultoportulae and ribs that radiate to the periphery of the diatom (Figure 5). The valve surface is decorated with pores, with an average perimeter of 125 nm, that increase in density from the centre of the diatom to the periphery (Figure 6). Conversely, the rib-like structures become less dense at the periphery. Scanning electron microscopy (SEM) micrographs revealed that the overall frustule morphology of *T. weissflogii* was preserved under multiple additions of TiBALDH over 192 hours (Figure 5). The resemblance observed by SEM was supported by images generated by transmission electron microscopy (TEM) with the pores decorating the valve face appearing unaltered (Figure 6a & 6b). However, further analysis was required to elucidate whether the architecture of the TiBALDH-modified frustules were completely analogous to the morphology described for the *T. weissflogii* cultured in Na_2SiO_3. For this purpose, the valve surface was subdivided into four concentric regions and extensive characterization of the pore size and radial pore distribution using TEM images was performed. Neither the pore size nor the pore density across the valve of TiBALDH-modified frustules were significantly different to those treated with Na_2SiO_3 (Figure 6c & 6d). The architectural parameters were further analysed using atomic force microscopy (AFM) analysis (Figure 7 & 8). The density of pores within Regions 2 and 3 of the valve surface were not statistically different between Na_2SiO_3 and TiBALDH diatoms (Figure 6b). A preliminary investigation comparing data generated by TEM and AFM was performed to ensure the accuracy of the data collected by AFM. The spacing from pore edge-to-edge from three separate sections of a TiBALDH-modified diatom in Regions 2 and 3 quantified from TEM data was 72 ± 3 nm, 73 ± 3 nm, and 68 ± 3 nm (Supplementary Figure 2). The average spacing from pore valley-to-valley in the same regions quantified from AFM data was 68 ± 3 nm (Supplementary Figure 2) in agreement with data from TEM. Further AFM analysis revealed that TiBALDH-modified diatoms did not differ from diatoms cultured in Na_2SiO_3 in parameters of pore valley-to-valley distance, pore depth, ironed surface area, spacing of the ribs, or rib height (Figure 8a–8e). However, there was an increase in the rib width (Figure 8f) in TiBALDH-modified diatoms as compared to those cultured in Na_2SiO_3. Previous studies have reported that the morphology of the precipitates obtained *in*

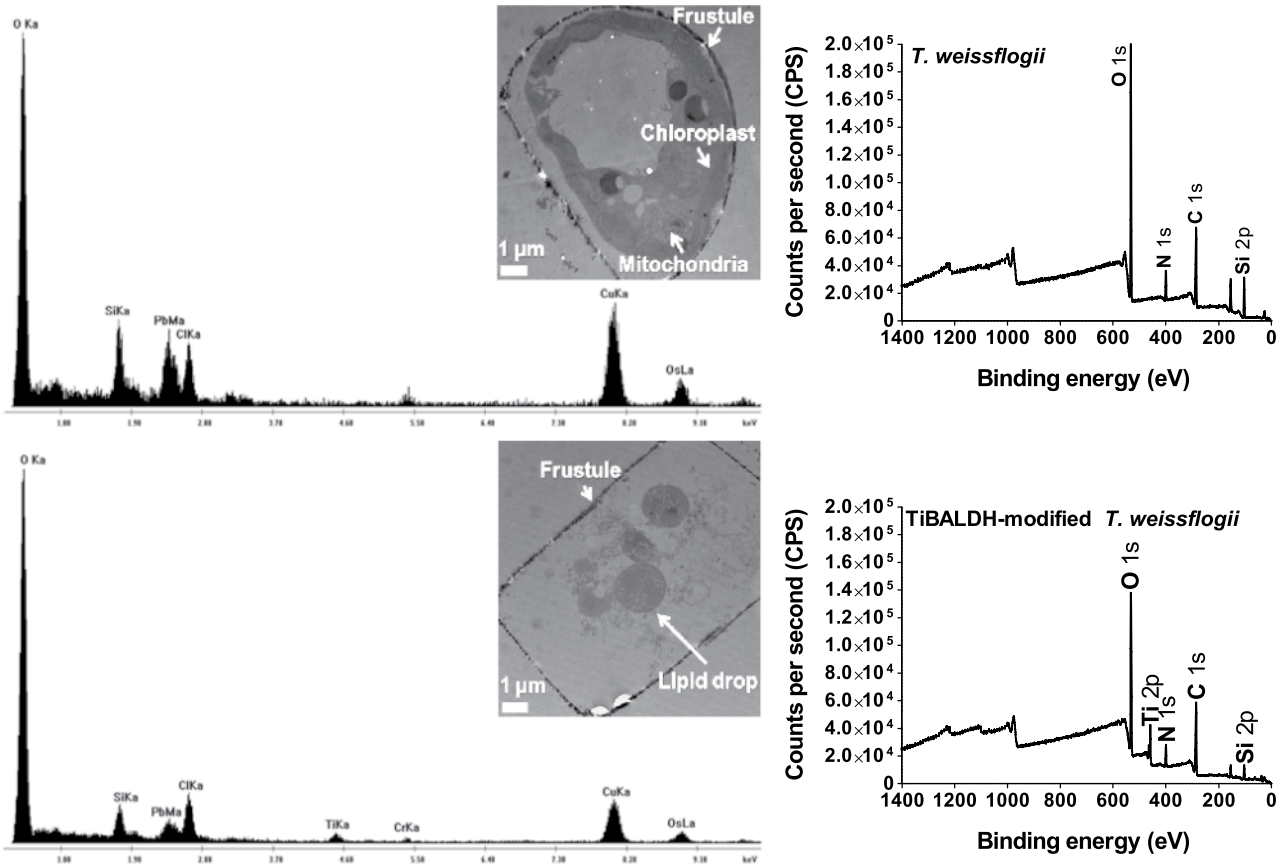

Figure 3 | Qualitative analysis of titanium in TiBALDH-modified *T. weissflogii*. (a & c) EDX-TEM spectra and micrograph of 90 nm cross sections of fixed *T. weissflogii* and TiBALDH-modified *T. weissflogii*. Arrows indicate cell organelles encased within the frustule (b & d) XPS spectra of *T. weissflogii* and TiBALDH-modified *T. weissflogii*. The chemical form of Si and Ti present is SiO_2 and TiO_2.

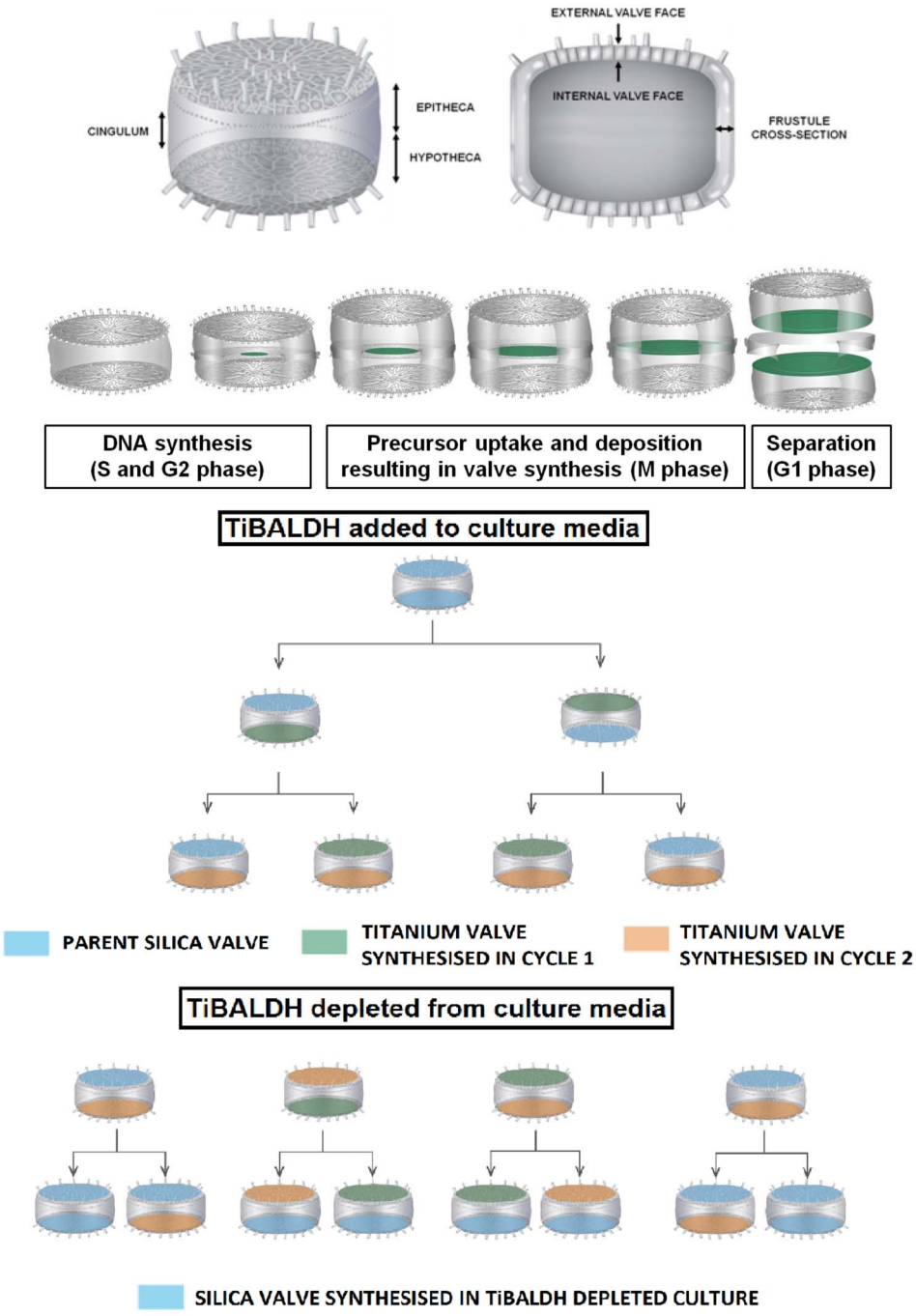

Figure 4 | Incorporation of Ti into the diatom during frustule synthesis. (a) The diatom is composed of an epitheca and hypotheca that fit together like a petri dish. Each theca is composed of the valve face (epivalve or hypovalve) and the valve mantle. The overlap region of the valves is surrounded by structures referred to as girdle bands and this region is referred to as the cingulum. A cross section of the diatom reveals that the pores present on the external valve face penetrate to the internal face. (b) Incorporation of Ti into both valves of the diatom frustule requires a minimum of two cell cycle divisions. The diatom cell cycle consists of an S phase where DNA synthesis occurs, followed by a gap in time (G2 phase). Upon silica uptake, two daughter cell protoplasts are synthesized in the silica deposition vesicle (SDV) of the mother cell before mitosis (M phase). This is followed by another gap (G1 phase) where daughter cells separate and growth via expansion of the girdle band occurs. (c) Depletion of TiBALDH in the culture media will lead to a decrease in Ti content. Failure to replenish TiBALDH in the culture media will result in decreased Ti content with successive cell divisions. Decaying diatoms or dissolution of silica from living diatoms in the culture media may provide a source of silica for uptake enabling continued cell divisions.

vitro exhibit significant differences depending on whether Na_2SiO_3 or TiBALDH was used as a precursor[12,15]. The type of silaffin involved in the precipitation[15], the secondary structure of the silaffin[27], the amino acid sequence of the long-chain polyamine[28], and the peptide sequence[29] are hypothesized to play a role in the morphologies of the precipitates obtained *in vitro*. Whether these factors influence the rib morphology of the frustules obtained in the culture medium that contains TiBALDH is unclear and further investigation will be required to elucidate this issue.

Novel properties of TiBALDH-modified *T. weissflogii*. In the present study, co-cultivation of TiBALDH-modified *T. weissflogii* in the presence of *Escherichia coli* (*E. coli*) provided interesting results. The model bacterial strain of choice *E. coli* was used in this

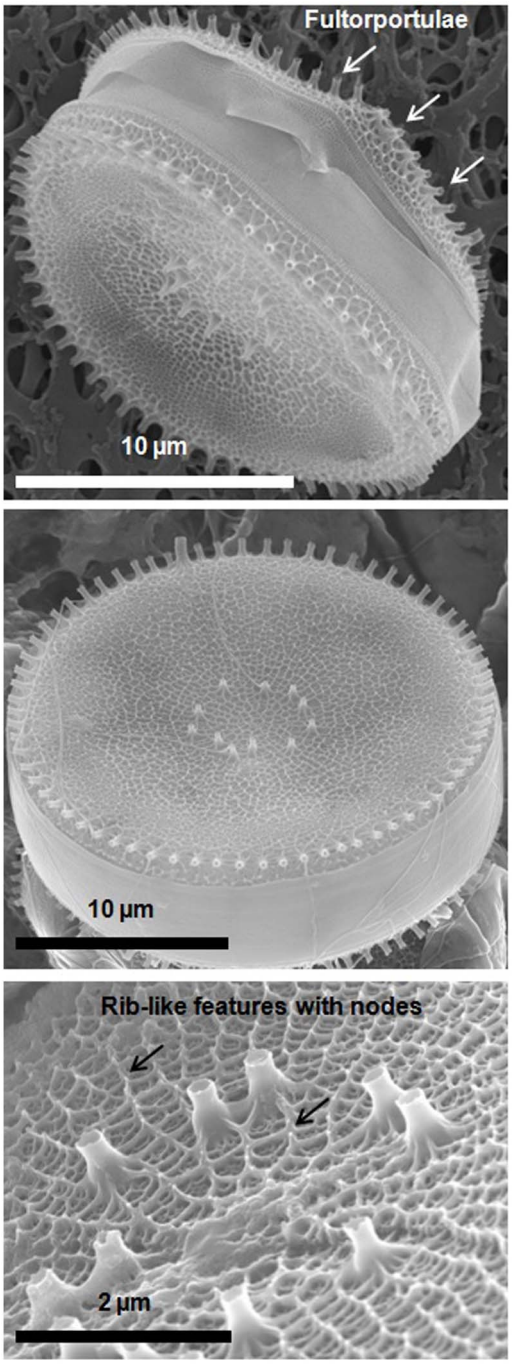

Figure 5 | The characteristic hierarchical architecture of the diatom is conserved in TiBALDH-modified *T. weissflogii*. Scanning electron microscopy images of *T. weissflogii* show that *T. weissflogii* is a centric diatom with highly intricate protrusions on the valve surface. Ribs radiate from the centre of the structure, underneath which the valve is decorated with openings. The images shown here are diatoms grown in the presence of (a) Na_2SiO_3 or (b) & (c) TiBALDH collected at 192 hours post inoculation following multiple addition of Na_2SiO_3 or TiBALDH at 48 hour intervals.

study. Cultures were inoculated in sterile de-ionised water so as to provide no nutrients to either diatom or bacteria. The abundance of either bacteria or diatom present was quantified over the time frame of the experiment. Co-cultures of (i) *T. weissflogii* with *E. coli* or (ii) TiBALDH-modified *T. weissflogii* with *E. coli* were studied with or without illumunation over a 24-hour period. Axenic cultures of (i) *T. weissflogii*, (ii) TiBALDH-modified *T. weissflogii*, and (iii) *E. coli* were studied under identical experimental conditions to serve as a control.

Both unmodified and TiBALDH-modified diatoms were capable of preserving the number of bacteria over the first six hours irrespective of exposure to UV light (Figure 9). These results are in agreement with what is known in the field, that diatoms tend to promote the growth of bacteria[30–33]. A close inspection of the changes after the first six hours revealed that there was a significant decay in the number of colonies in co-cultures of *E. coli* with TiBALDH-modified *T. weissflogii* following exposure to UV light. Any decay of *E. coli* in the presence of TiBALDH-modified diatoms disappeared when maintained in the dark. The profile of *E. coli* colony counts in the presence of unmodified *T. weissflogii* did not change under either light or dark settings demonstrating a slight decrease between 12 and 24 hours post inoculation. The decay of *E. coli* in co-cultures with diatoms has no precedent, and this is the first such observation reported to date. The decay of *E. coli* in the presence of TiBALDH-modified diatoms was

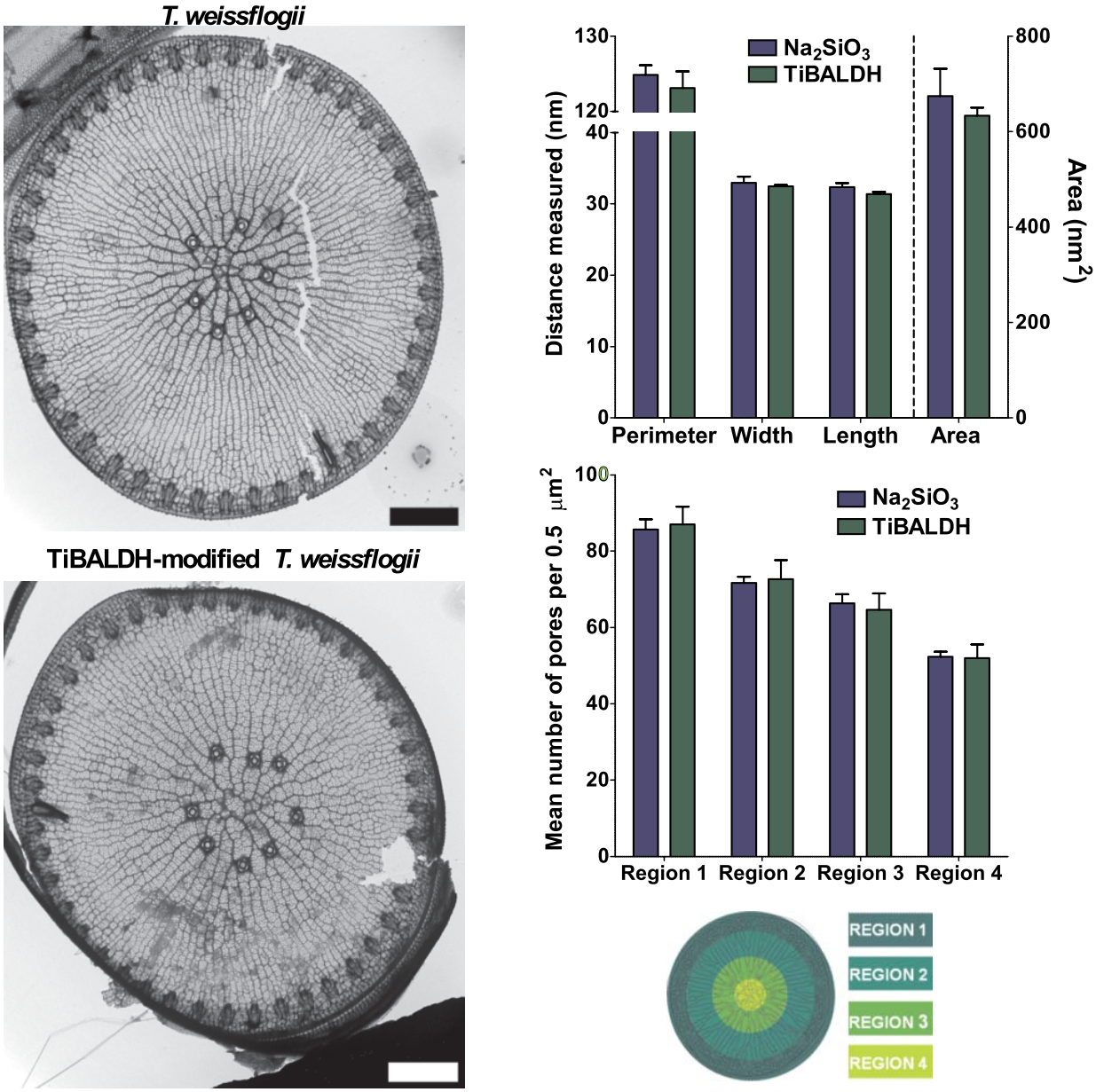

Figure 6 | The architectural properties related to the pores on the valve surface of *T. weissflogii* are unaltered in TiBALDH-modified diatoms. Transmission electron microscopy images of (a) *T. weissflogii* and (b) TiBALDH-modified *T. weissflogii*. Scale bar represents 2 µm. (c) Pore parameters of perimeter, width, length and area were not significantly different between Na_2SiO_3 and TiBALDH treated diatoms. (d) The pore distribution decreases in density from the periphery of the diatom to the centre of the diatom similarly for Na_2SiO_3 and TiBALDH treated diatoms. The schematic illustrates regions analysed on the valve surface with Region 4 represented in the centre of the valve. All data was generated from diatoms collected at 192 hours post inoculation following multiple addition of Na_2SiO_3 or TiBALDH at 0, 48, 96 and 144 hours post inoculation ($n = 3$ diatoms per culture, 3 cultures per treatment).

expected to be due to the photocatalytic activity of TiO_2 as it is absent in cultures maintained under dark settings.

The photocatalytic ability of cleaned TiBALDH-modified *T. weissflogii* frustules was also investigated. Degradation of methylene blue under UV light in the presence of either unmodified or modified diatoms was monitored. A decrease in the absorbance of the methylene blue solution at 656 nm was observed only in the presence of TiBALDH-modified diatoms following exposure to UV light (Supplementary Figure 3).

Discussion

The preservation of the diatom growth pattern upon the chemical modification of the culture medium is an aspect of paramount importance. Exposure of diatoms to sub-lethal doses of alternative precursors results in alterations to the architecture of the diatom, explained in part by interruptions to the processes within the silica deposition vesicle (SDV) and modification of cell organelles[34,35]. Accordingly, the threshold concentration of chemical entities that can be incorporated into the culture medium to modify the diatom morphology and/or composition must fulfil a delicate balance: sufficiently high that any modification is detectable, yet sufficiently low to avoid cytotoxic concentrations that alter diatom growth patterns. In this study, TiBALDH added to the culture at a final concentration of 200 µM met these criteria.

The increase in cell density observed in the presence of TiBALDH not only confirms that the presence of Ti does not adversely affect the growth pattern of *T. weissflogii*, but also suggests that Ti is capable of being incorporated into the diatom frustule by a metabolically

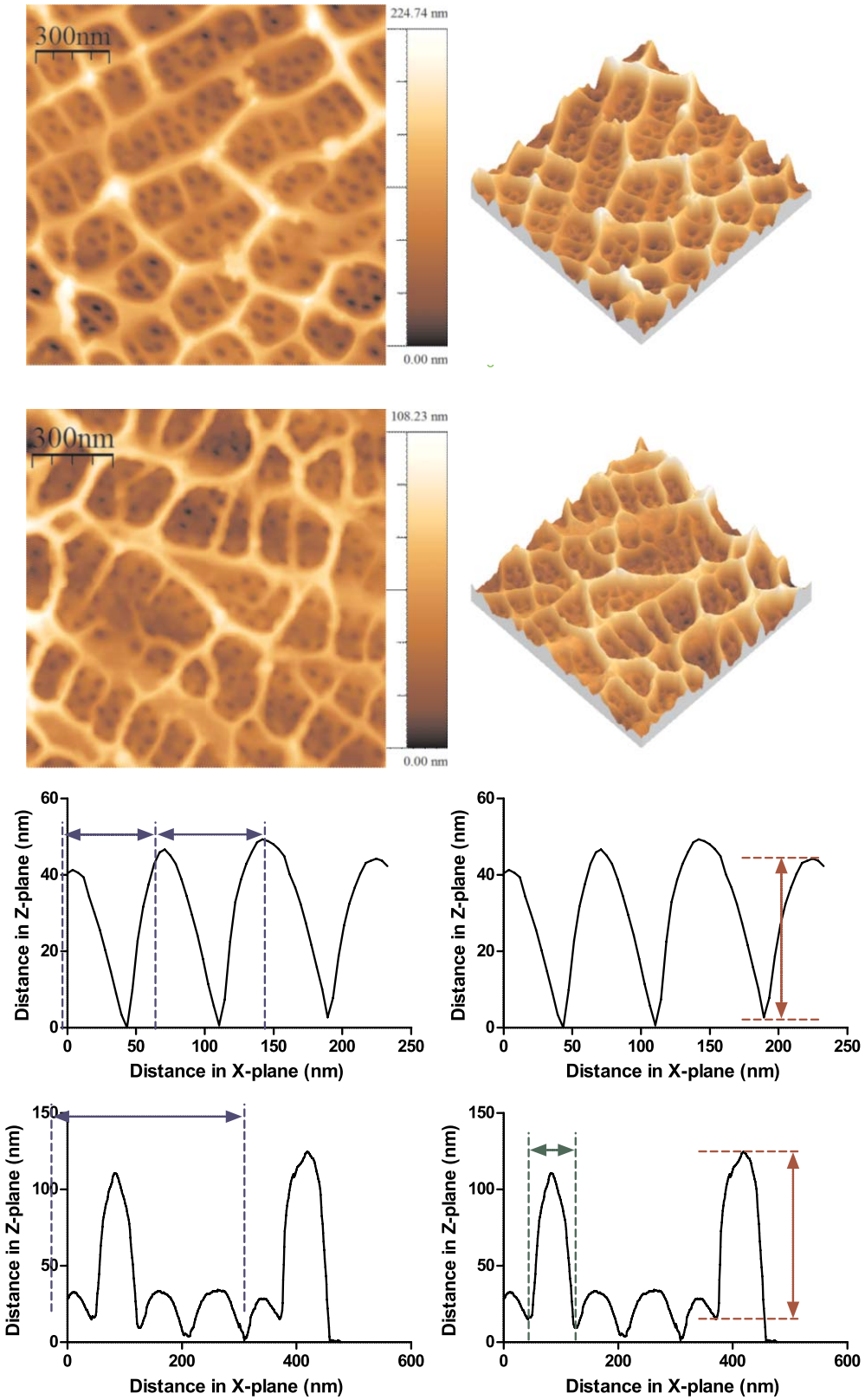

Figure 7 | Fine nodular features decorate the rib structure on the valve of *T. weissflogii*. The surface topography of (a) *T. weissflogii* and (b) TiBALDH modified *T. weissflogii* imaged by AFM reveals the fine structural details of the valve surface showing nodes decorating the ribs and the textured surface underneath the ribs. Images were generated from diatoms collected at 192 hours post inoculation following multiple addition of Na_2SiO_3 or TiBALDH at 0, 48, 96 and 144 hours post inoculation. (c) Measurements were collected in Regions 2 and 3 as defined in Figure 6d. The panel of graphs represent profiles taken on the valve surface depicting criteria for measurements of (i) valley-to-valley distance (ii) pore depth (iii) rib-to-rib distance (iv) rib width (green) and height (red).

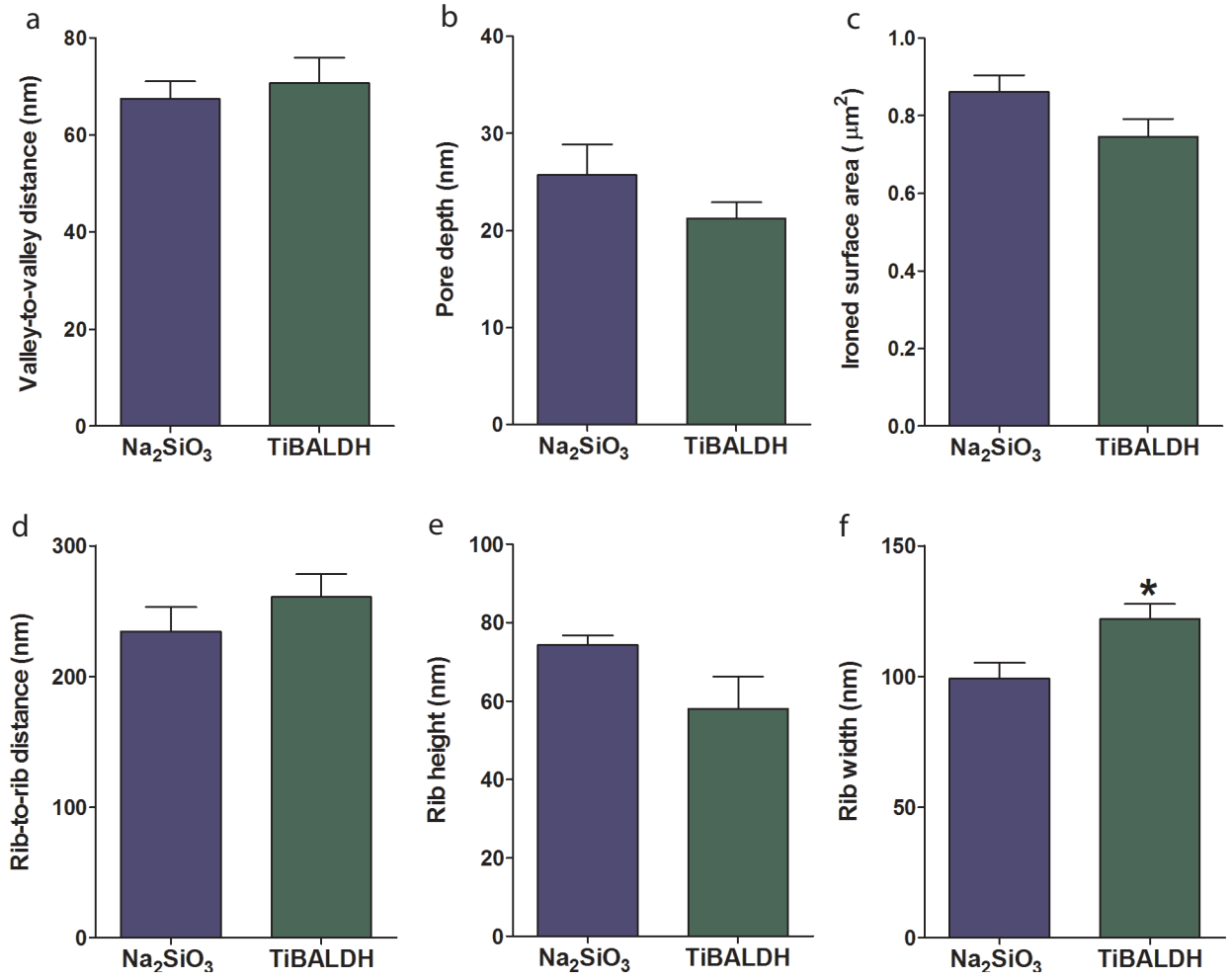

Figure 8 | Architectural parameters relating to the rib structure on the valve surface are altered in TiBALDH modified *T. weissflogii*. Data are quantified from AFM images and represented as mean ± sem ($n = 4$ diatoms per treatment). (a) Distance between neighbouring pores measured from valley-to-valley (b) Pore depth (c) Ironed surface area of a 0.5 μm^2 section on valve surface (d) Distance between neighbouring ribs measured from rib crest-to-crest (e) Rib height (f) Rib width, *t*-test revealed significant difference for Na_2SiO_3 vs TiBALDH $^*p < 0.05$. Data were generated from diatoms collected at 192 hours post inoculation following multiple addition of Na_2SiO_3 or TiBALDH at 0, 48, 96 and 144 hours post inoculation.

associated process. Further, exploration of the exact mechanism is required but is hampered by the lack of Ti specific inhibitors.

This Ti content achieved using TiBALDH is enhanced compared to that seen with $TiOSO_4$. However; the TiBALDH treatment was insufficient to create a fully SiO_2–depleted valve. Figure 4b illustrates the formation of new valves within the silica deposition vesicle in the parent diatom. Incorporation of the precursor requires uptake of the precursor into the parent diatom, deposition of the precursor within the SDV, followed by division of the parent diatom into two daughter diatoms. The daughter diatom consists of an epitheca composed of original material from the parent diatom and a hypotheca composed of material from the precursor. Incorporation of the precursor into both valves of the frustule requires a minimum of two cell cycles (Figure 4c). As additional Na_2SiO_3 was not added to TiBALDH treated cultures, one would expect the formation of six fully SiO_2–depleted frustules after three cell cycles from one parent SiO_2–diatom (Figure 4c). However, this was not observed experimentally.

Titanium dioxide particles have been shown to have bactericidal properties when irradiated with UV light[36–38], however this mechanism is a matter for discussion and possible suggestions including oxidation of intracellular enzymes leading to decreases in bacterial cell respiration and death[36], or disruption of the bacterial cell membrane leading to cell death[39]. Nonetheless, the generation of free radicals is the root cause of the bactericidal properties of TiO_2 particles. Irradiation of TiBALDH-modified *T. weissflogii* in co-culture with *E. coli* leads to a decrease in bacteria abundance. This behaviour is not observed in co-cultures of *T. weissflogii* and *E. coli*, and is expected to be due to photocatalysis of TiO_2. As an alternative to photocatalysis, it can be postulated that the difference between *E. coli* colony numbers in the presence of either unmodified or TiBALDH-modified diatoms under illumination is due to metabolic differences. However, the lack of an observed difference between the co-culture systems under dark conditions (Figure 9) does not support this idea, and indicates a photocatalytic mechanism underlying the differences observed under UV irradiation.

In summary, the use of TiBALDH as a precursor in diatom cultures allowed for a metabolic insertion of up to 14.2 ± 5.1 pg Ti per diatom valve. TiBALDH was chosen because of its stability in the culture medium, which is one of the critical issues that favours precursor uptake. Enhanced metabolic insertions were found with experimental conditions (*e.g.* multiple precursor additions) that prolong the exponential growth phase of the culture. The resemblance (in terms of both the pore size and distribution across the valve) between TiO_2-modified diatoms and regular diatoms suggests that, *in vivo*, silaffins and polyamines are determinants of TiBALDH precipitation into the patterned structure that characterizes diatom frustules. It is worth noting that the modification of the chemical composition of living diatoms have several implications. For

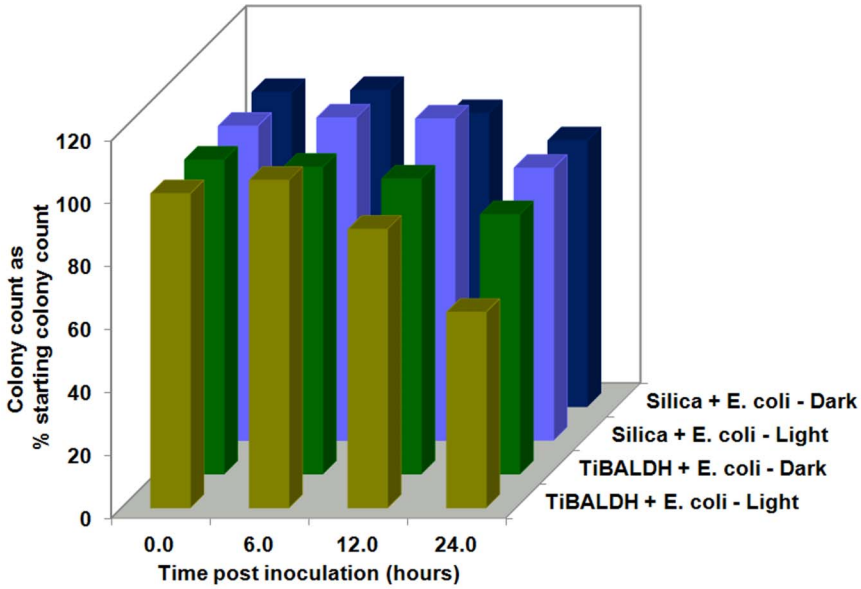

Figure 9 | TiBALDH-modified *T. weissflogii* decreases *E. coli* density under illumination but not under dark conditions. *E. coli* colony count expressed as a percentage of the starting colony count for co-cultures under illumination and dark conditions. Data are expressed as mean ± sem ($n = 3$).

instance, results generated in this work revealed how the suppression or the preservation of *T. weissflogii* in co-cultures with *E. coli* depended upon chemical composition. Moreover, co-cultures of TiBALDH-modified *T. weissflogii* diatoms exhibited an unprecedented decay of *E. coli* under illumination but not in dark conditions indicative of a certain photocatalytic activity originating from TiO_2 incorporated into the diatom frustules. While further investigation is clearly warranted to fully explore the potential of these features, the photocatalytic activity of living cultures of TiBALDH-modified *T. weissflogii* opens exciting possibilities in a number of applications. For instance, TiBALDH-modified diatoms can exert bactericidal effects. In this context it is worth noting that the TiO_2 concentration in the diatoms studied herein is nearly 1000-fold below that used in previous reports on photocatalytic TiO_2 particles exhibiting bactericidal effects[39].

Methods

Axenic *Thalassiosira weissflogii* cultures were grown in artificial seawater (ASW) prepared according to Berges *et al.*[40] enriched with Guillard's f/2 marine enrichment media without silicates (Sigma Aldrich) according to manufacturer recommendations. Cultures were silica depleted according to the procedure detailed by Hildebrand *et al.*[41] for a minimum of 24 hours before inoculation with the precursor. Following silica depeletion cultures were inoculated at 1×10^4 cells/mL or 5×10^4 cells/mL in a final volume of 200 ml. Cultures were grown in polystyrene tissue culture flasks.

Sodium metasilicate nonhydrate (Na_2SiO_3) or titanium bis(ammoniumlactacodihydroxide) (TiBALDH) were added to cultures at a final concentration of 200 μM and grown at a 14 hour : 10 hour light:dark cycle at a light intensity of 3000 lux and temperature range of 16–22°C. Multiple addition cultures received further additions of Na_2SO_3 or TiBALDH at a final concentration of 200 μM at 48, 96, and 144 hours. Cultures were collected at 192 hours post inoculation and diatoms cleaned according to procedure detailed in Supplementary Information. Cell density was monitored using a haemocytometer.

Determination of Ti content in cleaned frustules. SEM-EDX analysis was performed using Hitachi S-4700 SEM with INCA software (Oxford Instruments) to determine the Si and Ti content. Cleaned diatoms suspended in methanol were allowed to air dry on a carbon stub and were subsequently gold coated. Diatoms were analysed only if the valve view was clearly visible. Three diatoms per culture and a minimum of three cultures per treatment group were analysed. The ratio of Ti:Si was determined and represented as pg Ti per valve. The gradient of Ti across the diatom was analysed using the girdle view of the diatom. Nine diatoms were analysed with two spectra collected per diatom identified as girdle 1 and girdle 2. *t*-tests were performed to determine statistical difference between Si and Ti content across the girdle of the frustule. TEM-EDX analysis was performed on a 90 nm thick cross-sections of fixed *T. weissflogii* and fixed TiBALDH-modified *T. weissflogii* as detailed in Supplementary Information. ICP-MS analysis was performed using ICP-MS Elan 6000 Perkin Elmer-Sciex. Digestion of the samples was performed by microwave (high pressure microwave, model ETHOS SEL, Milestone) using equal part solution of HNO_3 and HF. XPS analysis was performed using the Kratos AXIS 165 spectrometer. Binding energies were referenced to the C 1 s line at 284.5 eV and 284.8 eV. Cleaned diatom samples were dried at 60°C for 48 hours. The dried sample was ground to a fine powder and dusted on to double sided adhesive tape for analysis.

Quantification of architectural parameters. Quantification of architectural parameters was performed on cleaned frustules grown in the presence of either Na_2SiO_3 or TiBALDH collected at 192 hours post inoculation following multiple addition of Na_2SiO_3 or TiBALDH at 48 hour intervals. TEM images of frustules were collected using Hitachi H-7500 TEM with AMT image capture software. Cleaned diatoms suspended in methanol were allowed to air dry on a copper grid. Pore parameters (perimeter, width, length and area) were quantified using ImageJ software. Five sections per diatom and five diatoms per culture were analysed. A minimum of three cultures per treatment group were analysed. Pore parameters were calculated as the mean ± sem per treatment ($n = 3$). Pore distribution across the valve surface was analysed using ImageJ software. The valve surface was divided into four discrete regions as illustrated in the schematic in Figure 6d. A minimum of eight sections measuring 0.5 μm^2 per region were analysed. Pore distribution was calculated as the mean ± sem per treatment ($n = 3$). AFM measurements were performed under ambient conditions in intermittent contact mode using a commercial AFM system (NanoWizard-II, JPK Instruments, Germany) coupled with an inverted optical microscope (Eclipse Ti-E, Nikon, Japan). Silicon cantilevers (spring constant, $k \sim 2.8$ N m^{-1} and resonance frequency, $f \sim 75$ kHz) with high aspect ratio (1:10 aspect ratio, tip radius < 3 nm), high density, diamond like carbon tips were used (MSS-FMR-13, Nanotools, Germany). Analysis of AFM images was performed using WSxM Software[42]. Sections within regions 2 and 3 as outlined in the schematic in Figure 7c were analysed. The criteria for measurements of valley-to-valley distance, pore depth, rib-to-rib distance, and rib width and rib height is illustrated in Figure 6c. *t*-tests were performed to determine statistical difference between Na_2SO_3 and TiBALDH treated cultures regarding architectural parameters.

Investigating the relationship between *T. weissflogii*/TiBALDH-modified *T. weissflogii* and *E.coli*. *Escherichia coli*, *T. weissflogii* and TiBALDH-modified *T. weissflogii* were prepared for the co-culture study as detailed in Supplementary Information. Six treatment groups were prepared to a final volume of 200 ml in sterile de-ionised water; (i) Water, (ii) *E. coli*, (iii) *T. weissflogii*, (iv) TiBALDH-modified *T. weissflogii*, (v) *T. weissflogii* + *E. coli*, (vi) TiBALDH-modified *T. weissflogii* + *E. coli*. Flasks were inoculated at diatom cell density of ca. 3×10^4 cells/mL and *E. coli* density of ca. 10^6 cfu/mL. Flasks were placed on a shaker and exposed to light (HALOLINE ECO 64695 from Osram) or covered with black cloth to eliminate exposure to light. 200 μl aliquots were removed at 0, 1.5, 3, 6, 12 and 24 hours post inoculation. Diatom cell counts were performed using a haemocytometer. Serial dilutions in sterile PBS were performed before plating 100 μl on LB agar plates. Plates were incubated at 37°C for 24 hours and colony counts recorded.

Investigating the degradation of methylene blue in the presence of *T. weissflogii* or TiBALDH-modified *T.weissflogii*. Cleaned *T. weissflogii* and TiBALDH-modified *T. weissflogii* were suspended in de-ionised water. Methylene blue dissolved in de-ionised water was added at a weight ratio of 0.1 mg dye:100 mg diatom. Six samples were prepared for both modified and unmodified diatoms. All samples were placed in

the dark for 1 hour afterwhich they were centrifuged at 2500 *g* for 20 minutes. The absorbance of the supernatent at 656 nm was measured to ensure that there was no difference between samples before the incubation period. Three samples for each unmodified and modified diatom were placed in the dark for 24 hours. The remaining samples were exposed to UV light at 365 nm. The absorbance of the supernatent was measured at 656 nm following the 24 hour incubation period.

1. Round, F. E., Crawford, R. M. & Mann, D. G. *The Diatoms: Biology and Morphology of the Genera.* (Cambridge University Press, New York, 1990).
2. Mann, S. *Biomineralization: Principles and Concepts in Bioinorganic Materials Chemistry* (Oxford University Press, New York, 2001).
3. Nassif, N. & Livage, J. From diatoms to silica-based biohybrids. *Chem. Soc. Rev.* **40**, 849–859 (2011).
4. Sandhage, K. H. *et al.* Novel, Bioclastic Route to Self-Assembled, 3D, Chemically Tailored Meso/Nanostructures: Shape-Preserving Reactive Conversion of Biosilica (Diatom) Microshells. *Adv. Mater.* **14**, 429–433 (2002).
5. Sandhage, K. H. *et al.* Merging Biological Self-Assembly with Synthetic Chemical Tailoring: The Potential for 3-D Genetically Engineered Micro/Nano-Devices (3-D GEMS). *Int. J. Appl. Ceram. Technol.* **2**, 317–326 (2005).
6. Holmes, S. M. *et al.* A novel porous carbon based on diatomaceous earth. *Chem. Commun.* 2662–2663 (2006).
7. Pérez-Cabero, M., Puchol, V., Beltrán, D. & Amorós, P. *Thalassiosira pseudonana* diatom as biotemplate to produce a macroporous ordered carbon-rich material. *Carbon* **46**, 297–304 (2008).
8. Vrieling, E. G. *et al.* Salinity-dependent diatom biosilicification implies an important role of external ionic strength. *Proc. Natl. Acad. Sci. U.S.A.* **104**, 10441–10446 (2007).
9. Davis, A. K. & Hildebrand, M. A self-propagating system for Ge incorporation into nanostructured silica. *Chem. Commun.* **37**, 4495–4497 (2008).
10. Qin, T., Gutu, T., Jiao, J., Chang, C. H. & Rorrer, G. L. Biological fabrication of photoluminescent nanocomb structures by metabolic incorporation of germanium into the biosilica of the diatom *Nitzschia frustulum*. *ACS Nano* **2**, 1296–1304 (2008).
11. Jeffryes, C., Gutu, T., Jiao, J. & Rorrer, G. L. Metabolic insertion of nanostructured TiO_2 into the patterned biosilica of the diatom Pinnularia sp. by a two-stage bioreactor cultivation process. *ACS Nano* **2**, 2103–2112 (2008).
12. Kröger, N., Deutzmann, R. & Sumper, M. Polycationic Peptides from Diatom Biosilica That Direct Silica Nanosphere Formation. *Science* **286**, 1129–1132 (1999).
13. Kröger, N., Lorenz, S., Brunner, E. & Sumper, M. Self-Assembly of Highly Phosphorylated Silaffins and Their Function in Biosilica Morphogenesis. *Science* **298**, 584–586 (2002).
14. Kröger, N., Deutzmann, R., Bergsdorf, C. & Sumper, M. Species-specific polyamines from diatoms control silica morphology. *Proc. Natl. Acad. Sci. U.S.A.* **97**, 14133–14138 (2000).
15. Kröger, N. *et al.* Bioenabled Synthesis of Rutile (TiO_2) at Ambient Temperature and Neutral pH. *Angew. Chem., Int. Ed.* **45**, 7239–7243 (2006).
16. Jantschke, A., Herrmann, A.-K., Lesnyak, V., Eychmüller, A. & Brunner, E. Decoration of diatom biosilica with noble metal and semiconductor nanoparticles (10 nm): Assembly, characterization, and applications. *Chem. Asian J.* **7**, 85–90 (2012).
17. Yu, Y., Addai-Mensah, J. & Losic, D. Chemical functionalization of diatom silica microparticles for adsorption of gold (III) ions. *J. Nanosci.Nanotech.* **11**, 10349–10356 (2011).
18. Yu, Y., Addai-Mensah, J. & Losic, D. Functionalized diatom silica microparticles for removal of mercury ions. *Sci. Technol. Adv. Mater.* **13**, 015008 (2012).
19. Wang, G. *et al.* Layer-by-layer dendritic growth of hyperbranched thin films for surface sol-gel syntheses of conformal, functional, nanocrystalline oxide coatings on complex 3D (bio)silica templates. *Adv. Funct. Mater.* **19**, 2768–2776 (2009).
20. De Luca, S., Ivo, R., De Mario, S., Alfredo, B. & Pasqualino, M. Marine diatoms as optical chemical sensors. *Appl. Phys. Lett.* **87**, 233902 (2005).
21. Weatherspoon, M. R. *et al.* Phosphor microparticles of controlled three-dimensional shape from phytoplankton. *J. Electrochem. Soc.* **153**, H34–H37 (2006).
22. Losic, D. *et al.* Surface functionalisation of diatoms with dopamine modified iron-oxide nanoparticles: Toward magnetically guided drug microcarriers with biologically derived morphologies. *Chem.Commun.* **46**, 6323–6325 (2010).
23. Aw, M. S., Simovic, S., Addai-Mensah, J. & Losic, D. Silica microcapsules from diatoms as new carrier for delivery of therapeutics. *Nanomedicine* **6**, 1159–1173 (2011).
24. Aw, M. S., Simovic, S., Yu, Y., Addai-Mensah, J. & Losic, D. Porous silica microshells from diatoms as biocarrier for drug delivery applications. *Powder Technol.* **223**, 52–58 (2012).
25. Lewin, J. C. Silicon metabolism in diatoms III: Respiration and silicon uptake in *Navicula pelliculosa*. *J. Gen. Physiol.* **39**, 1–10 (1955).
26. Azam, F., Hemmingsen, B. B. & Volcani, B. E. Role of Silicon Diatom Metabolism V. Silicic Acid Transport and Metabolism in the Heterotophic Diatom *Nitzschia alba*. *Arch. Microbiol.* **97**, 103–114 (1974).
27. Kharlampieva, E., Jung, C. M., Kozlovskaya, V. & Tsukruk, V. V. Secondary structure of silaffin at interfaces and titania formation. *J. Mater. Chem.* **20**, 5242–5250 (2010).
28. Cole, K. E. & Valentine, A. M. Spermidine and Spermine Catalyze the Formation of Nanostructured Titanium Oxide. *Biomacromolecules* **8**, 1641–1647 (2007).
29. Sewell, S. L. & Wright, D. W. Biomimetic synthesis of titanium dioxide utilizing the R5 peptide derived From *Cylindrotheca fusiformis*. *Chem. Mater.* **18**, 3108–3113 (2006).
30. Grossart, H. P. *et al.* between marine snow and heterotrophic bacteria: aggregate formation and microbial dynamics. *Aqua. Micro.Ecol.* **42**, 19–26 (2006).
31. Grossart, H. P., Czub, G. & Simon, M. Algae-bacteria interactions and their effects on aggregation and organic matter flux in the sea. *Environ. Microbiol.* **8**, 1074–1084 (2006).
32. Grossart, H. P., Tang, K. W., Kiørboe, T. & Ploug, H. Comparison of cell-specific activity between free-living and attached bacteria using isolates and natural assemblages. *FEMS Microbiol. Lett.* **266**, 194–200 (2007).
33. Gärdes, A., Iversen, M. H., Grossart, H.-P., Passow, U. & Ullrich, M. S. Diatom-associated bacteria are required for aggregation of *Thalassiosira weissflogii*. *ISME J.* **5**, 436–445 (2010).
34. Townley, H. E., Woon, K. L., Payne, F. P., White-Cooper, H. & Parker, A. R. Modification of the physical and optical properties of the frustule of the diatom *Coscinodiscus wailesii* by nickel sulfate. *Nanotechnology* **18**, 295101 (2007).
35. Saboski, E. M. Effects of mercury and tin on frustular ultrastructure of the marine diatom, *Nitzschia liebethrutti*. *Water, Air, Soil Pollut.* **8**, 461–466 (1977).
36. Matsunaga, T., Tomoda, R., Nakajima, T., Nakamura, N. & Komine, T. Continuous-sterilization system that uses photosemiconductor powders. *Appl. Environ. Microbiol.* **54**, 1330–1333 (1988).
37. Watts, R. J., Kong, S., Orr, M. P., Miller, G. C. & Henry, B. E. Photocatalytic inactivation of coliform bacteria and viruses in secondary wastewater effluent. *Water Res.* **29**, 95–100 (1995).
38. Marugán, J., van Grieken, R., Sordo, C. & Cruz, C. Intrinsic kinetic modeling with explicit radiation absorption effects of the photocatalytic oxidation of cyanide with TiO_2 and silica-supported TiO_2 suspensions. *App. Catal. B: Environ.* **85**, 48–60 (2008).
39. Maness, P. C. *et al.* Bactericidal activity of photocatalytic TiO(2) reaction: toward an understanding of its killing mechanism. *Appl. Environ. Microbiol.* **65**, 4094–4098 (1999).
40. Berges, J. A., Franklin, D. J. & Harrison, P. J. Evolution of an artificial seawater medium: improvements in enriched seawater, artificial water over the last two decades. *J. Phycol.* **37**, 1138–1145 (2001).
41. Hildebrand, M., Frigeri, L. G. & Davis, A. K. Synchronized growth of *Thalassiosira pseudonana* (Bacillariophyceae) provides novel insights into cell-wall synthesis processes in relation to the cell cycle. *J. Phycol.* **43**, 730–740 (2007).
42. Horcas, I. *et al.* WSXM: A software for scanning probe microscopy and a tool for nanotechnology. *Rev. Sci. Instrum.* **78**, 013705–013708 (2007).

Acknowledgments

The authors wish to thank the following for technical assistance: Mr. Daniel Kerr, Mr. Ambrose O'Halloran, Dr. Éadaoin Timmins, Mr. Pierce Lalor, Mr. Michael Coughlan at the National University of Ireland, Galway, Dr. Fathima Laffir, Dr. Calum Dickinson, and Dr. Hugh Geaney at the MSSI, University of Limerick, Inmaculada Rivas at SIdI, University Autonoma of Madrid, and Mr. Rafael Salas and Maarten H. Van Es. Illustrations were prepared by Maciek Doczyk and Marie Keely, Network of Excellence for Functional Biomaterials, National University of Ireland, Galway. This material is based upon works supported by the Science Foundation Ireland under Grant No. [07/SRC/B1163] and MINECO (MAT2009-10214 and MAT2012-34881). The AFM equipment used for this work was funded by Science Foundation Ireland (grant no. 07/IN1/B931).

Author contributions

Y.L., F.del M., D.P.F., and A.P. planned and designed experiments. Y.L. conducted experiments and data analysis. B.J.R. and P.D. assisted with TEM and AFM data analysis. Y.L., F.del M., D.P.F. and A.P. co-wrote paper.

Additional information

Supplementary information accompanies this paper at http://www.nature.com/scientificreports

Competing financial interests: The authors declare no competing financial interests.

How to cite this article: Lang, Y. *et al.* Integration of TiO_2 into the diatom *Thalassiosira weissflogii* during frustule synthesis. *Sci. Rep.* **3**, 3205; DOI:10.1038/srep03205 (2013).